Low-Cost Attitude and Heading Reference System Filter Using Complementary Method

Dr. Emad Natiq Abdulwahab
Mechanical Engineering Department, University of Technology/Baghdad.
Email:emadnaabd@yahoo.com.
Dr. Mohammed Idrees Mohsin
Mechanical Engineering Department, University of Technology/Baghdad.
Akeel Ali Wannas
Mechanical Engineering Department, University of Technology/Baghdad.
Email:yi3aaw@yahoo.com.

Received on:15/10/2014 & Accepted on:17/9/2015

ABSTRACT

This paper presents an orientation filter using complementary filter applicable to low-cost sensors based on micro electro-mechanical system (MEMS). The MEMS implementation incorporates magnetic distortion and gyroscope bias drift compensation. The filter uses a quaternion representation, allowing accelerometer and magnetometer data to be used in an analytically derived and optimized gradient-descent algorithm to compute the direction of the gyroscope measurement error as a quaternion derivative. The benefits of the filter are: (1) low scalar arithmetic operations for each filter update, (2) It is effective at low sampling rates; e.g. 10 Hz and (3) It contains adjustable parameters defined by observable system characteristics. The Performance was evaluated empirically using a commercially available orientation sensor and reference measurements of orientation obtained using an accurate servo motor (resolution < 0.3 degree). A simple calibration method is presented for the use of the electric-mechanical measurement equipment in this application. Results indicate that the filter achieves levels of accuracy exceeding that of the Kalman-based algorithm; < 0.821◦ for static RMS error and < 2.093◦ for dynamic RMS (Root Mean Square) error. The implications of the low computational load and ability to operate at low sampling rates use of MARG (Magnetic, Angular Rate, and Gravity) sensor arrays in real-time applications of limited power, processing resources or applications that demand extremely high sampling rates.

Keyword: AHRS, MEMS, Complementary Filter, Gyroscope, magnetometer, Accelerometer.

نظام تعيين الوضع والاتجاه بأستخدام المرشح التكميلي واطئ الكلفة

الخلاصة:

هذا المقال يقدم مرشح لاتجاه الاجسام باستخدام الطريقة التكميلية المطبق على أجهزة استشعار منخفضة التكلفة العاملة على الانظمة الكهروميكانيكية الدقيقة (MEMS) . تعاني اجهزة الاستشعار MEMS تشويه في الاتجاه المغناطيسي لمتحسس المجال المغناطيسي والتحيز في الجايروسكوب الذي يؤدي بدوره الى الانجراف. يستخدم مرشح الاتجاة التكميلي الذي هو موضوع البحث التمثيل المركب المتعدد، مما يتيح استخدام بيانات التسارع والمغنطيسية في حساب المشتقة من الناحية التحليلية والحل الامثل لخوارزمية تدرج النزول لحساب خطأ الاتجاه المحسوب من الجايروسكوب كمشتقة للمركب المتعدد. تكمن فوائد المرشح التكميلي بما يلي: (1)

https://doi.org/10.30684/etj.2015.116234
2412-0758/University of Technology-Iraq, Baghdad, Iraq

انخفاض العمليات الحسابية العددية لكل تحديث، (2) فعالة عند معدلات عينات منخفضة (3) يحتوي على معاملات قابلة للتعديل تحددها خصائص النظام. تم تقييم الأداء تجريبيا باستخدام اجهزة استشعار متاحة تجارية لتحديد وضعية الاتجاه ومرجعية قياس تم الحصول عليها من موتور كهربائي دقيق (ذات دقة <0.3 درجة). قدمت طريقة معايرة بسيطة تستخدم اجهزة كهروميكانيكبة في هذا التطبيق. تشير النتائج الى فعالية هذا المرشح الاتجاهي والتي تقارب من نتائج مرشح كالمان، حيث اعطت جذر متوسط مربع قيمة الخطأ بين 0.821 درجة للحالة الاستاتيكية و2.093 درجة للحالة الديناميكية. الآثار المترتبة على الحمل الحسابي المنخفض والقدرة على العمل في معدلات عينات منخفضة باستخدام MARG اعطى القابلية للعمل في ظروف المزامنة الحقيقية او اللحظية لموارد معالجة قليلة من ناحية المعالجات او الطاقة بالاضافة للعمل بمعدل عينات عالية جدا للتطبقات التي تحتاج الى ذلك، نظرا لقلة العمليات الحسابية لكل تحديث.

INTRODUCTION

In many engineering fields including: robotics [1], aerospace [2], navigation [3] human motion analysis [4] and machine interaction [5]. The orientation in three-dimensional space is one of the most significant pieces of information required for the navigation, guidance and control of that vehicle. The attitude and heading reference system (AHRS) is a general device to determine the orientation of a vehicle or an object which is attached to. Recently, investigations of attitude estimation with low-cost sensors based on micro electro-mechanical system (MEMS) have been conducted [6] [7]. Low-cost sensors suffer from large noise and errors, and this is the reason why the calibration and validation of the AHRS based on low-cost sensors are critical and necessary procedures to verify its accuracy and performance before its implementation.

A gyroscope measures the angular velocity which, if initial conditions are known, may be integrated over time to compute the sensor's orientation [8] [9]. Precision gyroscopes, ring laser for example, are too expensive and bulky for most applications and so less accurate MEMS devices are used in a majority of applications [10]. The integration of gyroscope measurement errors will lead to an accumulating error in the calculated orientation. Therefore, gyroscopes alone cannot provide an absolute measurement of orientation. An accelerometer and magnetometer will measure the earth's gravitational and magnetic fields respectively and so provide an absolute reference of orientation. However, they are likely to be subjected to high levels of noise; for example, accelerations due to motion will corrupt measured direction of gravity. The task of an orientation filter is to compute a single estimate of orientation through the optimal fusion of gyroscope, accelerometer and magnetometer measurements.

The Kalman filter [11] has become the accepted basis for the majority of orientation fitter algorithms [12] [13] [14] and commercial inertial orientation sensors; xsens [15], micro-strain [16], VectorNav [17], Intersense [18], PNI [19] and Crossbow [20] all produce systems founded on its use. The widespread use of Kalman-based solutions is a testament to their accuracy and effectiveness; however, they have a number of disadvantages. They can be complicated to implement which is reflected by the numerous solutions seen in the subject literature [12] [13] [14]. The linear regression iterations, fundamental to the Kalman process, demand sampling rates far exceeding the subject bandwidth; for example, a sampling rate between 512 Hz [15] and 30 kHz [16] may be used for a human motion caption application. The state relationships describing rotational kinematics in three-dimensions typically require large state vectors and an extended Kalman filter implementation [14] [21] to linearize the problem.

These challenges demand a large computational load for implementation of Kalman-based solutions and provide a clear motivation for alternative approaches. Many previous approaches to address these issues have implemented either fuzzy processing [1] [2] or fixed filters [22] to favor accelerometer measurements of orientation at low angular velocities and the integrated gyroscope measurements at high angular velocities. Such an approach is simple but may only be effective under limited operating conditions. Bachman et al [23] proposed an alternative approach where the filter achieves an optimal fusion of measurements data at all angular velocities. However, the process requires a least squares regression, which also brings in an associated computational load. Mahony et al [24] developed the complementary filter which is shown to be an efficient and effective solution; however, performance is only validated for an IMU (Inertial Measurement Units).

This paper introduces orientation filter that is applicable to MARG (Magnetic, Angular Rate, and Gravity) sensor arrays addressing issues of computational load and parameter tune. The filter employs a quaternion representation of orientation [14] to describe the coupled nature of orientations in three-dimensions and is not subjected to the problematic singularities associated with an Euler angle representation. A derivation [25] and empirical evaluation of the filter is presented. Its performance is benchmarked against an existing commercial filter and verified with electrical mechanical measurement system.

FILTER DERIVATION:

Orientation from gyroscope:

A three-axis gyroscope will measure the angular rate about the *x, y* and *z* axes of the senor frame, termed ω_x, ω_y and ω_z respectively. If these parameters (in rads^{-1}) are arranged into the vector $^S\omega$ defined by equation (**Error! Reference source not found.**), the quaternion derivative describing the rate of change of orientation of the earth frame relative to the sensor frame $^S_E\dot{q}$ can be calculated [25] as equation (1).

$$^S\omega = \begin{bmatrix} 0 & \omega_x & \omega_y & \omega_z \end{bmatrix} \quad \ldots(1)$$

$$^S_E\dot{q} = \frac{1}{2} {^S_E\hat{q}} \otimes {^S\omega} \quad \ldots(1)$$

The orientation of the earth frame relative to the sensor frame at time *t*, $^S_E q_{\omega,t}$, can be computed by numerically integrating the quaternion derivative $^S_E\dot{q}_{\omega,t}$ as described by equations (2) and (3) provided that initial conditions are known. In these equations, $^S\omega_t$ is the angular rate measured at time *t*, Δt is the sampling period and $^S_E\hat{q}_{est,t-1}$ is the previous estimate of orientation. The sub-script ω indicates that the quaternion is calculated from angular rates [25].

$$^S_E\dot{q}_{\omega,t} = \frac{1}{2} {^S_E\hat{q}_{est,t-1}} \otimes {^S\omega_t} \quad (2)$$

$$^S_E q_{\omega,t} = {^S_E\hat{q}_{est,t-1}} + {^S_E\dot{q}_{\omega,t}} \Delta t \quad (3)$$

Orientation from accelerometer and magnetometer:

In the context of an orientation estimation algorithm, it will initially be assumed that an accelerometer will measure only gravity and a magnetometer will measure only the earth's magnetic field. If the direction of an earth's field is known in the earth frame, a measurement of the field's direction within the sensor frame will allow an orientation of the sensor frame relative to the earth frame to be calculated. However, for any given measurement there will not be a unique sensor orientation solution, instead there will infinite solutions represented by all those orientations achieved by the rotation the true orientation around an axis parallel with the field. A quaternion representation requires a single solution to be found. This may be achieved through the formulation of an optimization problem where an orientation of the sensor ${}^S_E\hat{q}$, is found as that which aligns a predefined reference direction of the field in the earth frame ${}^E\hat{d}$, with the measured field in the sensor frame ${}^S S$; thus solving (4) where equation (5) defines the objective function [25].

$$\min_{{}^S_E\hat{q}\in\Re^4} f\left({}^S_E\hat{q},{}^E\hat{d},{}^S\hat{s}\right) \qquad \dots(4)$$

$$f\left({}^S_E\hat{q},{}^E\hat{d},{}^S\hat{s}\right)={}^S_E\hat{q}^*\otimes{}^E\hat{d}\otimes{}^S_E q-{}^S\hat{s} \qquad \dots(5)$$

Gradient descent algorithm is one of the simplest to both implement and compute. Equation (6) describes the gradient descent algorithm for n iterations resulting in an orientation estimation of ${}^S_E\hat{q}_{n+1}$ based on an 'initial guess' orientation ${}^S_E\hat{q}_0$ and a variable step-size μ. Equation (7) computes an error direction on the solution surface defined by the objective function, f, and its Jacobian, J [26].

$${}^S_E q_{k+1}={}^S_E q_k-\mu\frac{\nabla f\left({}^S_E\hat{q},{}^E\hat{d},{}^S\hat{s}\right)}{\left\|\nabla f\left({}^S_E\hat{q},{}^E\hat{d},{}^S\hat{s}\right)\right\|},\ k=0,1,2...n \qquad \dots.(6)$$

$$\nabla f\left({}^S_E\hat{q}_k,{}^E\hat{d},{}^S\hat{s}\right)=J^T\left({}^S_E\hat{q}_k,{}^E\hat{d}\right)f\left({}^S_E\hat{q}_k,{}^E\hat{d},{}^S\hat{s}\right) \qquad \dots.(7)$$

Equations (6) and (7) describe the general form of the algorithm applicable to a field predefined in any direction. However, if the reference direction of the field is defined to only have components within 1 or 2 of the principle axis of the earth coordinate frame then the equations simplify. An appropriate convention would be to assume that the direction of gravity defines the vertical, z axis as shown in equation (10). Substituting ${}^E\hat{g}$ and normalized accelerometer measurement ${}^S\hat{a}$ for ${}^E\hat{d}$ and ${}^S\hat{s}$ respectively, yields the simplified objective function and Jacobian defined by equations (11) and (12).

$$ {}_{E}^{S}\hat{q} = \begin{bmatrix} q_1 & q_2 & q_3 & q_4 \end{bmatrix} \qquad \ldots(8)$$

$$ {}^{E}g = \begin{bmatrix} 0 & 0 & 0 & 1 \end{bmatrix} \qquad \ldots(9)$$

$$ {}^{S}\hat{a} = \begin{bmatrix} 0 & a_x & a_y & a_z \end{bmatrix} \qquad \ldots(10)$$

$$ f_g\left({}_{E}^{S}\hat{q}_k, {}^{S}\hat{a}\right) = \begin{bmatrix} 2(q_2q_4 - q_1q_3) - a_x \\ 2(q_1q_2 - q_3q_4) - a_y \\ 2(0.5 - q_2^2 - q_3^2) - a_x \end{bmatrix} \qquad \ldots(11)$$

$$ J_g\left({}_{E}^{S}\hat{q}\right) = \begin{bmatrix} -2q_3 & 2q_4 & -2q_1 & 2q_2 \\ 2q_2 & 2q_1 & 2q_4 & 2q_3 \\ 0 & -4q_2 & -4q_3 & 0 \end{bmatrix} \qquad \ldots(12)$$

The earth's magnetic field can be considered to have components in one horizontal axis and the vertical axis [27].This can be represented by equation (14). Substituting ${}^{E}\hat{b}$ and normalized magnetometer measurement ${}^{S}\hat{m}$ for ${}^{E}\hat{d}$ and ${}^{S}\hat{s}$ respectively, yields the simplified objective function and Jacobian defined equations (15) and (16).

$$ {}^{S}\hat{b} = \begin{bmatrix} 0 & b_x & 0 & b_z \end{bmatrix} \qquad \ldots(13)$$

$$ {}^{S}\hat{m} = \begin{bmatrix} 0 & m_x & m_y & m_z \end{bmatrix} \qquad \ldots(14)$$

$$ f_b\left({}_{E}^{S}\hat{q}, {}^{E}\hat{b}, {}^{S}\hat{m}\right) = \begin{bmatrix} 2b_x(0.5 - q_3^2 - q_4^2) + 2b_z(q_2q_4 - q_1q_3) - m_x \\ 2b_x(q_2q_3 - q_1q_4) + 2b_z(q_1q_2 + q_3q_4) - m_y \\ 2b_x(q_1q_3 + q_2q_4) + 2b_z(0.5 - q_2^2 - q_3^2) - m_z \end{bmatrix} \qquad \ldots(15)$$

$$ J_g\left({}_{E}^{S}\hat{q}, {}^{E}\hat{b},\right) = \begin{bmatrix} -2b_zq_3 & 2b_zq_4 & -4b_xq_3 - 2b_zq_1 & -4b_xq_4 + 2b_zq_2 \\ -2b_xq_4 + 2b_zq_2 & 2b_xq_3 + 2b_zq_1 & 2b_xq_2 + 2b_zq_4 & -2b_xq_1 + 2b_zq_3 \\ 2b_xq_3 & 2b_xq_4 - 4b_zq_2 & 2b_xq_1 - 4b_zq_3 & 2b_xq_2 \end{bmatrix} \qquad \ldots(16)$$

As has already been discussed, the measurement of gravity or the earth's magnetic field alone will not provide a unique orientation of the sensor. To do so, the measurements and reference directions of both fields may be combined as described by equations (17) and (18). Whereas the solution surface created by the objective functions in equations (12) and (16) have a global minimum defined by a line, the solution surface define by equation (18) has a minimum define by a single point, provided that $b_x \neq 0$.

$$ f_{g,b}\left({}_{E}^{S}\hat{q}, {}^{S}\hat{a}, {}^{E}\hat{b}, {}^{S}\hat{m}\right) = \begin{bmatrix} f_g\left({}_{E}^{S}\hat{q}, {}^{S}\hat{a}\right) \\ f_{g,b}\left({}_{E}^{S}\hat{q}, {}^{E}\hat{b}, {}^{S}\hat{m}\right) \end{bmatrix} \qquad \ldots(17)$$

$$ J_{g,b}\left({}_{E}^{S}\hat{q}, {}^{E}\hat{b}\right) = \begin{bmatrix} J^T{}_g\left({}_{E}^{S}\hat{q}\right) \\ J^T{}_{g,b}\left({}_{E}^{S}\hat{q}, {}^{E}\hat{b}\right) \end{bmatrix} \qquad (18)$$

A conventional approach to optimization would require multiple iterations of equation (6) to be computed for each new orientation and corresponding sensor measurements. However, it is acceptable to compute iteration per time sample provided that the convergence rate of the estimated orientation governed by μ_t is equal or greater than the rate of change of physical orientation. Equation (19) calculates the estimated orientation ${}^S_E q_{\nabla,t}$ computed at time t based on a previous estimate of orientation ${}^S_E \hat{q}_{est,t-1}$ and the objective function error ∇f defined by sensor measurements ${}^S\hat{a}_t$ and ${}^S\hat{m}_t$ sampled at time *t*. The form of ∇f is chosen according to the sensors in use, as shown in equation (20). The subscript ∇ indicates that the quaternion is calculated using the gradient descent algorithm

$$ {}^S_E q_{\nabla,t} = {}^S_E \hat{q}_{est,t-1} - \mu_t \frac{\nabla f}{\|\nabla f\|} \quad \ldots(19)$$

$$\nabla f = \begin{cases} J_g^T\left({}^S_E \hat{q}_{est,t-1}\right) f_g\left({}^S_E \hat{q}_{est,t-1}, {}^S\hat{a}_t\right) \\ J^T_{g,b}\left({}^S_E \hat{q}_{est,t-1}, {}^E\hat{b}\right) f_{g,b}\left({}^S_E \hat{q}_{est,t-1}, {}^E\hat{b}, {}^S\hat{m}_t\right) \end{cases} \quad \ldots(20)$$

An appropriate value of μ_t is that which ensures the convergence rate of ${}^S_E q_{\nabla,t}$ is limited to the physical orientation rate as this avoids overshooting due an unnecessarily large step size. Therefore μ_t can be calculated as equation (21) where Δt is the sampling period, ${}^S_E \dot{q}_{\omega,t}$ is the rate of change of orientation measured by gyroscopes and α is an augmentation of μ to account for noise in accelerometer and magnetometer measurements [25].

$$\mu_t = \alpha \left\| {}^S_E \dot{q}_{\omega,t} \right\| \Delta t, \ \alpha > 1 \quad \ldots(21)$$

Filter fusion algorithm:

An estimated orientation of the sensor frame relative to the earth frame ${}^S_E q_{est,t}$, is obtained through the fusion of the orientation calculations, ${}^S_E q_{\omega,t}$ and ${}^S_E q_{\nabla,t}$; calculated using equations (3) and (19) respectively. The fusion of ${}^S_E \hat{q}_{\omega,t}$ and ${}^S_E q_{\nabla,t}$ is described by equation (22) where t and $(1-\gamma_t)$ are weights applied to each orientation calculation [25].

$${}^S_E q_{est,t} = \gamma_t \, {}^S_E q_{\nabla,t} + (1-\gamma_t) {}^S_E q_{\omega,t} , \ 0 \le \gamma_t \le 1 \quad (22)$$

An optimal value of t can be defined as that which ensures the weighted divergence of ${}^S_E q_\omega$ is equal to the weighted convergence of ${}^S_E q_\nabla$. This is represented by equation (23) where $\mu_t/\Delta t$ the convergence rate of ${}^S_E q_\nabla$ and β is the divergence rate of ${}^S_E q_\omega$ expressed as the magnitude of a quaternion derivative corresponding to the gyroscope measurement error. Equation (23) can be rearranged to define γ_t as equation (24).

$$(1-\gamma_t)\beta = \gamma_t \frac{\mu_t}{\Delta t} \quad \ldots(23)$$

$$\gamma_t = \frac{\beta}{\frac{\gamma_t}{\Delta t} + \beta} \quad \ldots(24)$$

Equations (22) and (24) ensure the optimal fusion of ${}^S_E q_{\omega,t}$ and ${}^S_E q_{\nabla,t}$ assuming that the convergence rate of ${}^S_E q_{\nabla}$ governed by α is equal or greater than the physical rate of change of orientation. Therefore α has no upper bound. If α is assumed to be very large then μ_t, defined by equation (21), also becomes very large and the orientation filter equations simplify. A large value of μ_t used in equation (19) means that ${}^S_E \hat{q}_{est,t-1}$ becomes negligible and the equation can be re-written as equation (25).

$${}^S_E q_{\nabla,t} \approx -\mu_t \frac{\nabla f}{\|\nabla f\|} \quad \ldots(25)$$

The definition of γ_t in equation (24) also simplifies as the β term in the denominator becomes negligible and the equation can be rewritten as equation (26). It is possible from equation (26) to also assume that $\gamma_t \approx 0$.

$$\gamma_t \approx \frac{\beta \Delta t}{\mu_t} \quad \ldots(26)$$

Substituting equations (3), (25) and (26) into equation (22) directly yields equation (27). It is important to note that in equation (27), t has been substituted as both as equation (25) and 0

$${}^S_E q_{est,t} = \frac{\beta \Delta t}{\mu_t}\left(-\mu_t \frac{\nabla f}{\|\nabla f\|}\right) + (1-0)\left({}^S_E \hat{q}_{est,t-1} + {}^S_E \dot{q}_{\omega,t} \Delta t\right) \quad \ldots(27)$$

Equation (27) can be simplified to equation (28) where ${}^S_E \dot{q}_{est,t}$ the estimated rate of change of orientation is defined by equation (29) and ${}^S_E \dot{\hat{q}}_{\in,t}$ is the direction of the error of ${}^S_E \dot{q}_{est,t}$ defined by equation (30).

$${}^S_E q_{est,t} = {}^S_E \hat{q}_{est,t-1} + {}^S_E \dot{q}_{est,t}\, \Delta t \quad \ldots(28)$$

$${}^S_E \dot{q}_{est,t} = {}^S_E \dot{q}_{\omega,t} - \beta\, {}^S_E \dot{\hat{q}}_{\in,t} \quad \ldots(29)$$

$${}^S_E\dot{\hat{q}}_{\in,t} = \frac{\nabla f}{\|\nabla f\|} \qquad \ldots(30)$$

It can be seen from equations (27) to (30) that the filter calculates the orientation ${}^S_E q_{est}$ by numerically integrating the estimated orientation rate ${}^S_E \dot{q}_{est}$. The filter computes ${}^S_E \dot{q}_{est}$ as the rate of change of orientation measured by the gyroscopes, ${}^S_E \dot{q}_{\omega}$, with the magnitude of the gyroscope measurement error, β, removed in the direction of the estimated error, ${}^S_E\dot{\hat{q}}_{\in}$, computed from accelerometer and magnetometer measurements.

Magnetic distortion compensation:

Measurements of the earth's magnetic field will be distorted by the presence of ferromagnetic elements in the vicinity of the magnetometer. Investigations into the effect of magnetic distortions on an orientation sensor's performance have shown that substantial errors may be introduced by sources including electrical appliances, metal furniture and metal structures within a buildings construction [28]. Sources of interference fixed in the sensor frame, termed hard iron biases, can be removed through calibration [29]. Sources of interference in the earth frame, termed soft iron, cause errors in the measured direction of the earth's magnetic field. Declination errors, those in the horizontal plane relative to the earth's surface, cannot be corrected without an additional reference of heading. Inclination errors, those in the vertical plane relative to the earth's surface, may be compensated for as the accelerometer provides an additional measurement of the sensor's attitude.

The measured direction of the earth's magnetic field in the earth frame at time t, ${}^E\hat{h}_t$, can be computed as the normalized magnetometer measurement, ${}^S\hat{m}_t$, rotated by the estimated orientation of the sensor provided by the filter, ${}^S_E\hat{q}_{est,t-1}$; as described by equation (31). The effect of an erroneous inclination of the measured direction earth's magnetic field, ${}^E\hat{h}_t$, can be corrected if the filter's reference direction of the earth's magnetic field, ${}^E\hat{b}_t$, is of the same inclination. This is achieved by computing ${}^E\hat{b}_t$ as ${}^E\hat{h}_t$ normalized to have only components in the earth frame x and z axes; as described by equation (32).

$${}^E\hat{h}_t = \begin{bmatrix} 0 & h_x & h_y & h_z \end{bmatrix} = {}^S_E\hat{q}_{est,t-1} \otimes {}^S\hat{m}_t \otimes {}^S_E\hat{q}^*_{est,t-1} \qquad \ldots(31)$$

$${}^E\hat{b}_t = \begin{bmatrix} 0 & \sqrt{h_x^2 + h_y^2} & 0 & h_z \end{bmatrix} \qquad \ldots(32)$$

Compensating for magnetic distortions in this way ensures that magnetic disturbances are limited to only affect the estimated heading component of orientation. The approach also eliminates the need for the reference direction of the earth's magnetic field to be predefined; a potential disadvantage of other orientation filter designs [14]. Figure 1 shows a block diagram representation of the complete filter implementation for a MARG sensor array

Filter gains:

The filter gain β represents all mean zero gyroscope measurement errors, expressed as the magnitude of a quaternion derivative. The sources of error include: sensor noise, signal aliasing, quantization errors, calibration errors, sensor miss-alignment, and sensor axis non-orthogonally and frequency response characteristics. It is convenient to define β using the angular quantity ω_β, where $\tilde{\omega}_\beta$ represents the estimated mean zero gyroscope measurement error of each axis. Using the relationship described by equation (1), β may be defined by equation (33) where $\hat{q}$ is any unit quaternion.

$$\beta = \left\| \frac{1}{2}\hat{q} \otimes \begin{bmatrix} 0 & \tilde{\omega}_\beta & \tilde{\omega}_\beta & \tilde{\omega}_\beta \end{bmatrix} \right\| = \sqrt{\frac{3}{4}}\tilde{\omega}_\beta \qquad \ldots(33)$$

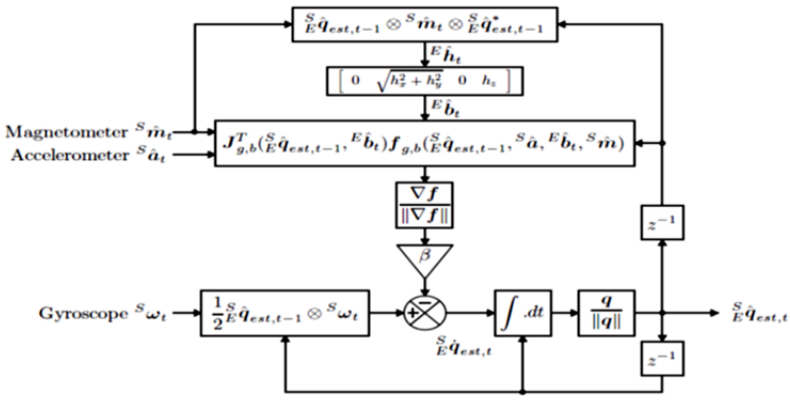

Figure (1). Block diagram representation of the complete orientation estimation algorithm including magnetic distortion compensation

EXPERIMENTATION:

Design of Rotating Platform:

In order to validate the performance of the AHRS, a platform with one axis of rotation and exact orientation feedback is developed. The magnetometer is sensitive to those components with ferromagnetic materials and the wires with high current, the platform should be fabricated with nonmagnetic materials. Moreover, the test section, to which the sensors are attached, should be far away from these sources of interference. Therefore, all the components of the platform are fabricated with plastic, as shown in Figure 2.

The validation of filter depends on error between real and filter output angles in real time test. In order to achieve this requirement one axis of rotation was used to drive a servo motor. One HItec HS-311 motor was installed on the yaw axis. This servo motor is produced by the Robotics and capable of providing the angular position feedback with the resolution of 0.29°, which is depicted in the datasheet. From the datasheet, in our case the maximum angular rate is 400°/s at 6 volt. The range of the angular position feedback of the servo motor is 0-180°. In order to achieve the heading angle validation, one incremental encoder with the resolution of

1024 counts/rev was setup to the z-axis of the platform; hence the range of yaw angular position feedback increases to 180°. This servo motor is controlled by receiving commands from the PC via the UART interface to Servo controller. The received commands include the target angular position and the angular rate.

This platform can be test anther two angles pitch and roll, by changing position of sensors on servo motor.

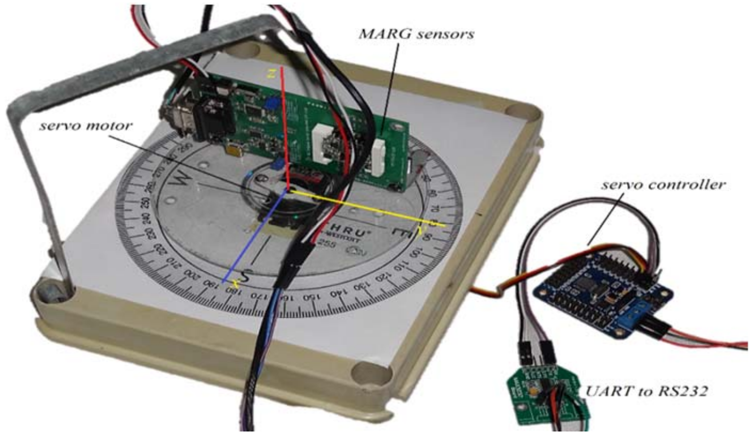

a. Image for platform test

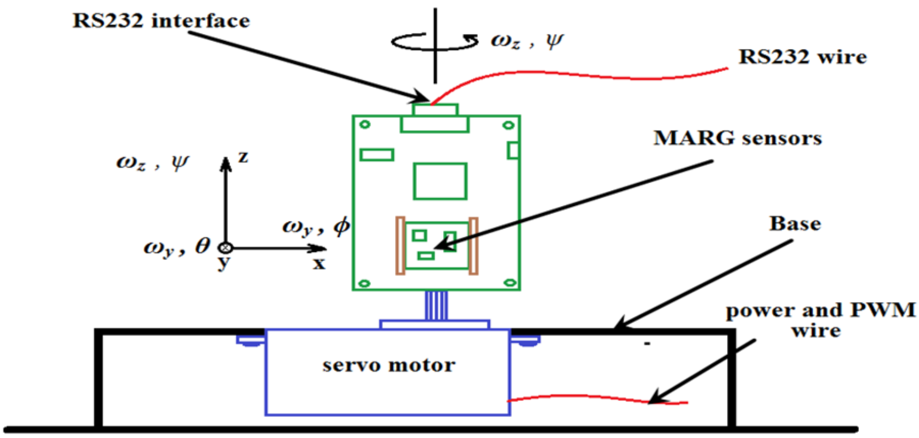

b. Schematic diagram of platform test

Figure (2). Orientation measurement platform

Results and Filter Validation:

The purpose of the validation of the AHRS filter is to check the reliability and the calibrated sensors (from sensors datasheet) and data fusion algorithm. With these calibrated parameters of the sensors and the AHRS, the estimated angle errors can be eliminated or reduced to an acceptable region. Two tests, static test and dynamic test, were conducted to demonstrate the AHRS validation in this study.

It is common [14] through [18] to quantify orientation sensor performance as the static and dynamic RMS (Root-Mean-Square) errors in the decoupled Euler parameters describing the pitch, roll, and yawing components of an orientation. Pitch, φ, roll, θ and yawing, ψ correspond to rotations around the sensor frame x, y, and z axis respectively. An Euler angle representation has the advantage that the decoupled angles may be more easily interpreted or visualized. The disadvantage of an Euler representation is that it fails to described the coupling between each of the parameters and will subject to large and erratic errors if the Euler angle sequence reaches a singularity.

Figures (3, 4 and 5) show typical experimental results for complementary filter MARG implementation. In each figure, the two traces of the upper plot represent the real measured angle by potentiometer of servo motor, and filter estimated angle. The two traces of the lower plot represent the calculated error in each of the estimated angles

The static and dynamic RMS values of φ_ε, θ_ε, and ψ_ε were calculated when a static state was assumed and the measured corresponding angular rate was < 5°/s, and a dynamic state was ≥ 5°/s. This threshold was chosen to be suitably high enough above the noise floor of the data. Each RMS value was calculated for the period of time framing only the rotation sequence of the corresponding Euler parameter; as indicated in figures 3, 4 and 5. The results are summarized in table 1. Each value represents the mean of experiments. Results indicate that the proposed filter achieves good levels of accuracy to use it in application like robot or UAV.

Results in table 1 indicate that the proposed filter achieves good accuracy comparing with Kalman-based algorithm [25].

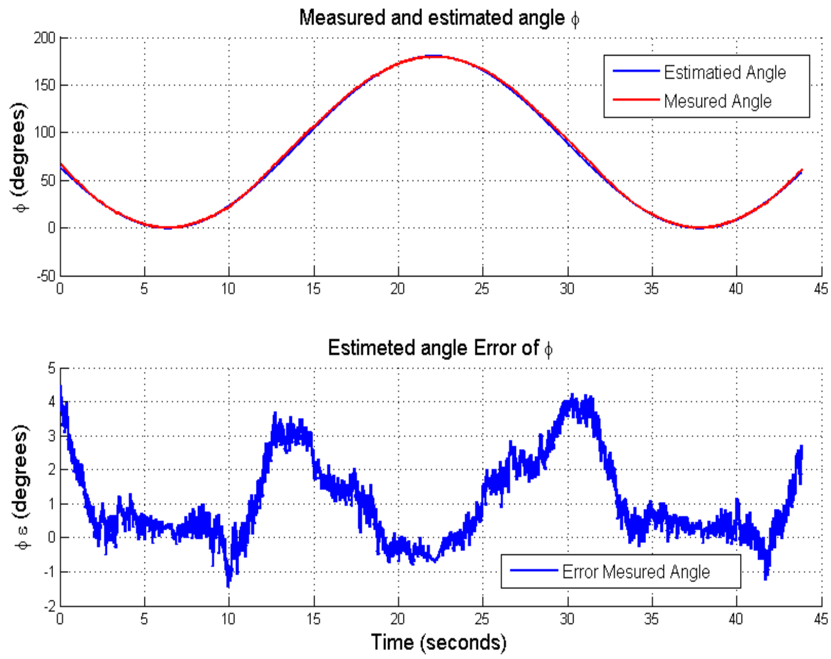

Figure (3): Measured and estimated angle φ and error

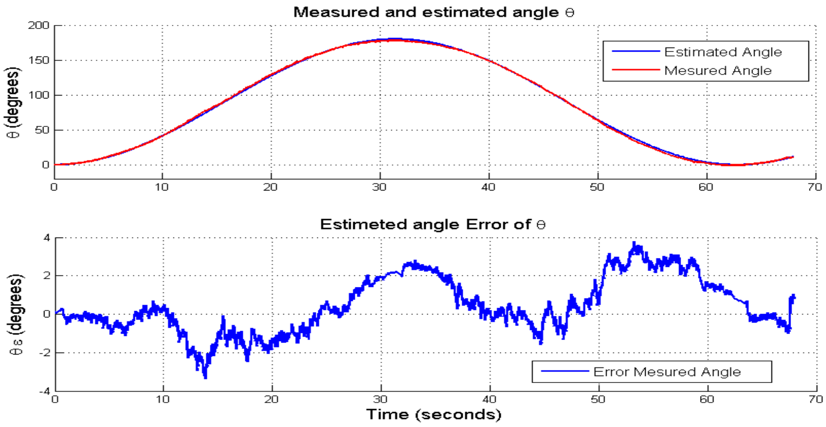

Figure (4): Measured and estimated angle θ and error

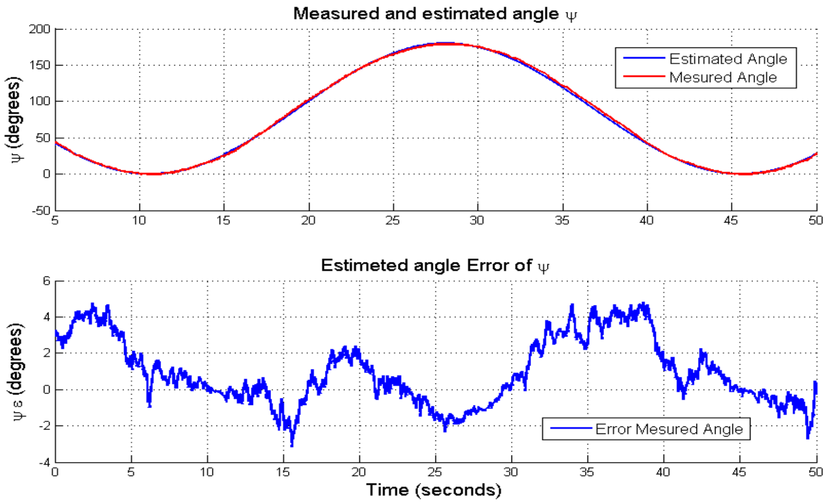

Figure (5): Measured and estimated angle ψ and error

CONCLUSIONS:

In this orientation filter, applicable to both Inertial Measurement Units and Magnetic, Angular Rate, and Gravity sensor arrays that significantly ameliorate the computational load and parameter tuning burdens associated with conventional Kalman-based approaches. The filter is based on a Newton optimization using an analytic formulation of the gradient that is derived from a quaternion representation of motion.

The advantages of this filter are: 1. Analytic derivation of the Jacobian matrix, which eliminate computational load, allowing implementation at very high sampling frequencies with low processing speed. 2. The need to tune only filter gains β, defined by the gyroscope measurement error. The filter derivation, magnetic distortion and gyroscope bias drift compensation, and experimental testing have been detailed. Empirical testing and benchmarking have shown that the filter performs as well as a high quality commercial Kalman-based system, even with a full order of magnitude in reduction of sampling rate. The filter is both simple to implement and simple to tune. The implications of the low computational load and ability to operate at low sampling rates open a very wide range of new opportunities for the use of Inertial Measurement Units and MARG sensor arrays in real-time applications. Applications where limited power or processing resources may be available are particularly well suited for the new filter. The filter also has great potential to alleviate computational load for applications that demand extremely high sampling rates.

Table (1): Static and dynamic RMS error

	No.	Euler Angle	RMS (dynamic)[°]	RMS (static) [°]
Current Filter	1	φ	1.6105	0.823
	2	θ	1.4815	0.8041
	3	ψ	2.093	1.0318
Kalman Filter	1	φ	0.769	0.789
	2	θ	0.847	0.819
	3	ψ	1.344	1.11

REFERENCES:

[1] L. Ojeda and J. Borenstein, "FLEXnav: fuzzy logic expert rule-based position estimation for mobile robots on rugged terrain," in Robotics and Automation, Proceedings. ICRA '02. IEEE International Conference on, vol. 1, May 11-15, 2002, pp. 317-322.

[2] Sung Kyung Hong, "Fuzzy logic based closed-loop strapdown attitude system for unmanned aerial vehicle (uav)," Sensors and Actuators A: Physical, vol. 107, no. 2, pp. 109 - 118, 2003.

[3] S. Beauregard, "Omnidirectional pedestrian navigation for first responders," in In Proc. 4th Workshop on Positioning, Navigation and Communication WPNC '07, March 22-22, 2007, pp. 33-36.

[4] Huiyu Zhou and Hu. Huosheng, "Human motion tracking for rehabilitation-A survey," Biomedical Signal Processing and Control, vol. 3, pp. 1 - 18, 2008.

[5] E. A. Heinz, K. S. Kunze, M. Gruber, D. Bannach, and P. Lukowicz, "Using wearable sensors for real-time recognition tasks in games of martial arts - an initial experiment," in In Proc. IEEE Symposium on Computational Intelligence and Games, May 22-24, 2006, pp. 98-102.

[6] M. Wang, Y.C. Yang, R.R. Hatch, and Y.H. Zhang, "Adaptive filter for a miniature MEMS based attitude and heading reference system," in Proceedings of IEEE Position Location and Navigation Symposium, Monterey, CA, USA, April 26–29, 2004, pp. 193–200.

[7] R. Zhu, D. Sun, Z.Y. Zhou, and D.Q. Wang, "A linear fusion algorithm for attitude determination using low cost MEMS-based sensors," Measurement, vol. 40, pp. 322–328, 2007.

[8] J. E. Bortz, "A new mathematical formulation for strapdown inertial navigation," Aerospace and Electronic Systems, IEEE Transactions on, vol. AES-7, no. 1, pp. 61-66, 1971.

[9] M. B. Ignagni, "Optimal strapdown attitude integration algorithms," In Guidance, Control, and Dynamics, vol. 13, no. 363-369, 1990.

[10] N. Yazdi, F. Ayazi, and K. Najafi, "Micromachined inertial sensors,"

Proceedings of the IEEE, vol. 86, no. 8, pp. 1640-1659, August 1998.

[11] R. E. Kalman, "A new approach to linear filtering and prediction problems," Journal of Basic Engineering, vol. 82, pp. 35-45, 1960.

[12] E. Foxlin, "Inertial head-tracker sensor fusion by a complementary separate-bias kalman filter," In Proc. Virtual Reality Annual International Symposium the IEEE, vol. 267, pp. 185-194, March 30-April 3, 1996.

[13] H. J. Luinge, P. H. Veltink, and C. T. M. Baten, "Estimation of orientation with gyroscopes and accelerometers," in In Proc. First Joint [Engineering in Medicine and Biology 21st Annual Conf. and the 1999 Annual Fall Meeting of the Biomedical Engineering Soc.] BMES/EMBS Conference, vol. 2, October 13-16, 1999, p. 844.

[14] J. L. Marins, Xiaoping Yun, E. R., R. B. Bachmann, and M. J. Zyda, "An extended kalman filter for quaternion-based orientation estimation using marg sensors," in In Proc. IEEE/RSJ International Conference on Intelligent Robots and Systems, volume 4, October 29-November 3, 2001, pp. 2003-2011.

[15] Xsens Technologies, B.V. MTi and MTx User Manual and Technical Documentation. Pantheon 6a, 7521 PR Enschede, The Netherlands., May 2009.

[16] Micro Strain Inc, 3DM-GX3 -25 Miniature Attitude Heading Reference Sensor. 459 Hurricane Lane, Suite 102, Williston, VT 05495 USA, 1.04 edition., 2009.

[17] VectorNav Technologies, "LLC. VN -100 User Manual. College Station, TX 77840 USA, preliminary edition," , 2009.

[18] InterSense, Inc. InertiaCube2+ Manual. 36 Crosby Drive, Suite 150, Bedford, MA 01730, USA, 1.0 edition., 2008.

[19] PNI Sensor Corporation, "Space point Fusion. 133 Aviation Blvd, Suite 101, Santa Rosa, CA 95403-1084 USA.,".

[20] Crossbow Technology, "Inc. AHRS400 Series User's Manual. 4145 N. First Street, San Jose, CA 95134, rev. c edition, February 2007.," in .

[21] A. M. Sabatini, "Quaternion-based extended kalman filter for determining orientation by inertial and magnetic sensing," Biomedical Engineering, IEEE, vol. 53, no. 7, pp. 1346-1356, July 2006.

[22] R. A. Hyde, L. P. Ketteringham, S. A. Neild, and R. J. S. Jones, "Estimation of upper-limb orientation based on accelerometer and gyroscope measurements," Biomedical Engineering, IEEE, vol. 55, no. 2, pp. 746-754, February 2008.

[23] E. R. Bachmann, Xiaoping Yun, and C. W. Peterson, "An investigation of the effects of magnetic variations on inertial/magnetic orientation sensors," in In Proc. IEEE International Conference on Robotics and Automation ICRA '04, volume 2, pages 1115-1122, April 2004.

[24] R. Mahony, T. Hamel, and J.M. Pimlin, "Nonlinear complementary filters on the special orthogonal group," Automatic Control, IEEE, vol. 53, no. 5, pp. 1203 - 1218, June 2008.

[25] Madgwick O. H., Harrison J.L., and Vaidyanathan Ravi, "Estimation of IMU and MARG orientation using a gradient descent algorithm," in IEEE International Conference on Rehabilitation Robotics. Rehab Week Zurich, ETH Zurich Science City, Switzerland, June 29 - July 1, 2011.

[26] Joseph M. Cooke, Michael J. Zyda, David R. Pratt, and Robert B. Mcghee,

"Npsnet: Flight simulation dynamic modelling using quaternions," Presence, vol. 1, pp. 404-420, 1992.

[27] J. A. Jacobs,.: The earth's core, vol. 37 of International geophysics series. Academic Press, 2 ed., 1987.

[28] E. R. Bachmann et al., "Orientation tracking for humans and robots using inertial sensors," in In Proc. IEEE International Symposium on Computational Intelligence in Robotics and Automation CIRA '99, November 8-9, 1999, pp. 187-194.

[29] J. F. Vasconcelos, G. Elkaim, C. Silvestre, P. Oliveira, and B. Cardeira, "A geometric approach to strapdown magnetometer calibration in sensor frame," in In Navigation, Guidance and Control of Underwater Vehicles, volume 2, 2008.